Available online at www.sciencedirect.com
ScienceDirect
Proceedings of the Combustion Institute xxx (2010) xxx–xxx
Proceedings of the Combustion Institute
www.elsevier.com/locate/proci

Chemical kinetics of copper oxide reduction with carbon monoxide

Eli A. Goldstein *, Reginald E. Mitchell

High Temperature Gasdynamics Laboratory, Thermosciences Group, Mechanical Engineering Department, Stanford University, Palo Alto, CA 94305, United States

Abstract

In order to assess the potential for using copper oxide as the oxygen source in chemical looping combustion with coal, a study was undertaken to characterize the reaction rates of copper oxide with carbon monoxide, a major coal partial oxidation product. In the study, CO oxidation experiments were performed in a pressurized thermogravimetric analyzer (TGA) with copper II (CuO) and copper I oxide (Cu_2O). In these experiments, about 25 mg of CuO or Cu_2O particles having diameters less than 125 μm were placed on the balance pan of the TGA and mixtures of 1.6% CO in N_2 were admitted into the reaction chamber, which was maintained at selected temperatures between 473 and 773 K. The measured thermograms were used to develop a chemical reaction mechanism and associated kinetic parameters to described CO oxidation with copper oxide. The reaction mechanism takes into account CO adsorption at copper sites, CO surface migration, and CO_2 desorption. Calculations employing the mechanism indicate that the overall reaction rate becomes mass transport limited for copper oxide particles larger than 125 μm in diameter, exposed to 100% CO at temperatures above 873 K. The reaction mechanism reveals a reaction order of 0.7 with respect to the CO mole fraction and an overall activation energy of 20 kJ/mol and 25 kJ/mol, respectively, for the reduction of CuO and Cu_2O to Cu. Calculated results support an earlier hypothesis that under the conditions examined, there are two pathways for CuO reduction to Cu, one cascading ($CuO \rightarrow Cu_2O \rightarrow Cu$) and the other direct ($CuO \rightarrow Cu$). Our results indicate that chemical looping combustion of coal employing CuO as the oxygen carrier will not be limited by chemical reaction rates.

Keywords: Chemical looping combustion; Oxidation with copper oxide; Carbon monoxide oxidation

1. Introduction

Since coal is the cheapest and most abundant fuel in the world, it has become the primary energy source used for electric power generation. In the United States, 51% of electricity originates from coal-fired power plants and in China, 75% of electricity is produced from burning coal [1]. As such, it is likely that coal will continue to be utilized in such a manner until non-fossil-fuel based technologies for electric power generation are commercially proven and in relatively widespread use.

"Clean coal" technologies have been developed to the point where the emissions of NO_x, SO_x, particulate matter, and mercury from present-day coal-fired power plants are below regulated levels. Presently, CO_2 emissions are not regulated. Since

* Corresponding author.
E-mail address: eagoldst@stanford.edu (E.A. Goldstein).

1540-7489/$ - see front matter © 2010 The Combustion Institute. Published by Elsevier Inc. All rights reserved.
doi:10.1016/j.proci.2010.06.080

Please cite this article in press as: E.A. Goldstein, R.E. Mitchell, *Proc. Combust. Inst.* (2010), doi:10.1016/j.proci.2010.06.080

CO_2 is a greenhouse gas and may be influencing the climate, it is prudent to remove it from power plant exhaust streams so as not to release it to the atmosphere. There are three pathways for enabling CO_2 sequestration: post-combustion, pre-combustion and oxyfuel combustion. Chemical looping combustion (CLC) is one promising oxyfuel combustion approach to CO_2 capture [2–7].

In CLC, an oxygen carrier, typically a metal oxide such as iron III oxide (Fe_2O_3) or copper II oxide (CuO), is circulated between a fuel reactor and an air reactor to transfer the oxygen necessary for fuel combustion. In the fuel reactor, the fuel is oxidized to CO_2 and H_2O and the metal oxide is reduced to the pure metal (or to a lower oxidation state). In the air reactor, the metal (or the lower oxidation state metal oxide) is oxidized back to its fully oxidized state.

In our investigation of CLC, we have selected CuO as the oxygen carrier. Based on literature surveys and thermodynamic analyses of potential CLC systems, in comparison to several other potential oxygen carriers (Fe_2O_3, NiO, BaO_2, Mn_2O_3, and SrO_2), CuO exhibits advantages with respect to the fuel-to-metal oxide mass ratio required for complete combustion, bed operating temperatures, toxicity, availability, handling, and cost [8]. Our overall efforts are directed at applying CLC technology to coal-fired and biomass-fired electric power plants. Consequently, we are concerned with the oxidation rates of these solid fuels with CuO. However, before solid fuel oxidation rates can be quantified with respect to temperature, pressure and reactive gas concentration, the rates of oxidation of CO, H_2 and CH_4 with CuO must be characterized.

Several studies aimed at understanding the oxidation characteristics of CuO have been undertaken due primarily to the catalytic activity of copper [9–16]. Experimental results have indicated that CuO catalytic activity proceeds through a reduction–oxidation (redox) reaction scheme and that CO oxidation via CuO proceeds through one of two dominant reaction pathways: $CuO \rightarrow Cu_2O \rightarrow Cu$ or $CuO \rightarrow Cu$ [9,13,15–17]. The actual pathways for reduction are complex and depend on a number of factors including the (i) creation of sites for CO adsorption, (ii) migration of CO on the surface, (iii) removal of oxygen from the copper oxide surface, (iv) migration of oxygen from the bulk to the surface, (v) growth or nucleation of suboxides and the reduced metal, and (vi) formation and removal of CO_2 [13]. Over a range of reaction conditions, the overall CuO reduction rate cannot be described using a single *n*th order kinetic expression [13]. Our objectives herein are to develop a reaction mechanism and associated kinetic parameters that can be used to predict CuO oxidation behaviors over the range of temperatures, pressures and compositions established in CLC systems.

2. Experimental approach

Copper II oxide of 99.99% purity was purchased from Sigma–Aldrich and copper I oxide of purity 99.9% was purchased from Alpha Aesar. To ensure that the thermogravimetric experiments were chemically controlled, the CuO particles were sieved to obtain particles in the 75–106 and 106–125 μm size ranges for testing. The Cu_2O particles as received were less then 30 μm. As such no sieving was performed to further refine the Cu_2O particle size distribution. The distributions for each size range of CuO particles were measured using a Coulter Multisizer. Despite the sieving of the CuO particles, there were still a large number of particles having diameters less than 30 μm. The size distribution of the Cu_2O particles could not be measured with the Coulter Multisizer since the Cu_2O particles are hydrophobic, causing them not to disperse in the instrument's electrolyte solution. To estimate an average size distribution, a scanning electron microscope (SEM, FEI XL30 Sirion SEM) was used to examine the particles. Measurement software was used to estimate a mean size (12 μm) and standard deviation (6 μm) for the Cu_2O particles.

The unreacted and reacted CuO and Cu_2O particles were also examined with an SEM and qualitatively analyzed via X-ray diffraction spectroscopy (using a PANalytical X'Pert XRD). The SEM images shown in Fig. 1 illustrate the morphological change in the copper oxide particles as a result of heating to 573 K. The unreacted CuO particles consist of nodules less than about 10 μm in size fused together. This morphology is likely a consequence of the manner in which the particles were manufactured. The nodules are not as evident in the particles after heat treatment. They seem to have coalesced, resulting in a particle with a rough, pitted surface. Measurements of the surface areas of the as received copper oxide and elemental copper particles were performed in our pressurized thermogravimetric analyzer (TGA), and both resulted in specific surface areas of about 1 m^2/g. Additionally, several surface area measurements were made after heating the CuO particles to 773 K and then after subsequent reaction with 1.6% CO in N_2 at 773 K. The mass specific surface area upon heating and then heating with chemical reaction was 40 m^2/g and 90 m^2/g respectively. This indicates that during heat-up and through reduction, the surface area increases. Surface area changes have been observed previously with redox reactions involving copper oxides [18,19]. The Brunauer–Emmett–Teller (BET) [20] approach was used in the analysis of gas adsorption weight data to determine the specific surface areas of CuO particles during reduction. Carbon dioxide was used as the adsorption gas, and adsorption tests were performed at 296 K and 10 atm. A value of 22.2 $Å^2$ was used for the

Please cite this article in press as: E.A. Goldstein, R.E. Mitchell, *Proc. Combust. Inst.* (2010), doi:10.1016/j.proci.2010.06.080

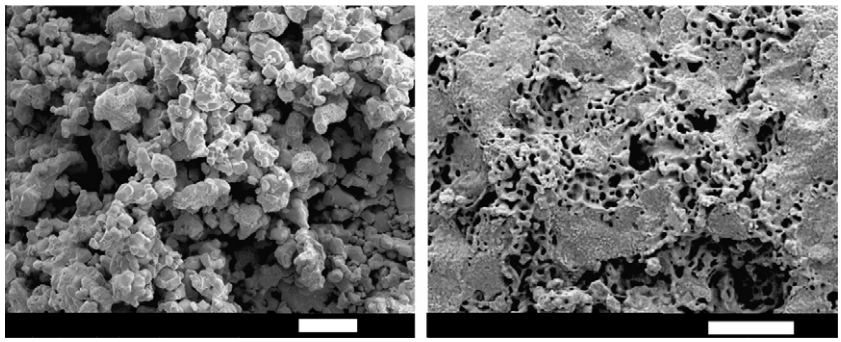

Fig. 1. SEM images of unreacted CuO particles (left) and CuO particles heated to 573 K (right) in nitrogen (white bar in each image represents 5 μm).

molecular cross section of CO_2 [21]. A description of the technique can be found elsewhere [22].

X-ray diffraction tests were used to identify the copper oxide species present in particles during a given experiment. Shown in the left panel of Fig. 2 are the XRD patterns from the unreacted copper oxide sample used in the experiments along with reference XRD patterns for CuO. Shown in the right panel are the XRD patterns from a partially reduced CuO sample (actually obtained in some of our experiments with corn stover as the fuel, under ramped temperature conditions) along with reference XRD patterns for Cu_2O. These data sets suggest the metal oxide reduction sequence of CuO to Cu_2O to Cu. Such a cascading of the copper valence during conversion has also been observed [9,13,15,16].

Based on the volume-to-external surface ratio, the mean radius of pores inside both the CuO and Cu_2O particles was estimated to be 0.006 μm. Pores as large as 0.5 μm were noted in some of our SEM images of the particles (see Fig. 1). Using a tap density technique [23], the apparent densities of the CuO and Cu_2O particles were determined to be 3.66 and 5.0 g/cm^3, respectively. Assuming true densities of 6.0 and 6.3 g/cm^3, respectively, for CuO and Cu_2O, particle porosities were estimated to be 0.42 for CuO and 0.17 for Cu_2O.

Carbon monoxide oxidation tests were performed in the TGA in order to determine the intrinsic chemical reactivity of CuO and Cu_2O. In our experimental procedure, 20–30 mg of CuO or Cu_2O particles were placed in the TGA balance pan and the particles were exposed to nitrogen at 298 K for 120 min before the temperature was increased to the specified reaction temperature (473, 573, 673 or 773 K). The particles experienced a dwell time of 60 min in nitrogen at the test temperature before the reactive gas was introduced into the reaction chamber. Weight change in the specified gaseous environment was monitored. The measured thermograms (mass (m) versus time (t) data) were used to derive specific conversion rate profiles ($1/m\ dm/dt$ versus t), which were analyzed in order to determine the rates of the rate-limiting reactions that control the overall conversion rate of the copper oxide to Cu during oxidation of CO.

3. Theoretical approach

Based on the physical characteristics of the particles used in the experiments, diffusion limited overall conversion rates (mass conversion rates per unit external surface area) for selected particle sizes were calculated for the conditions established in the reaction chamber of the TGA. The diffusion

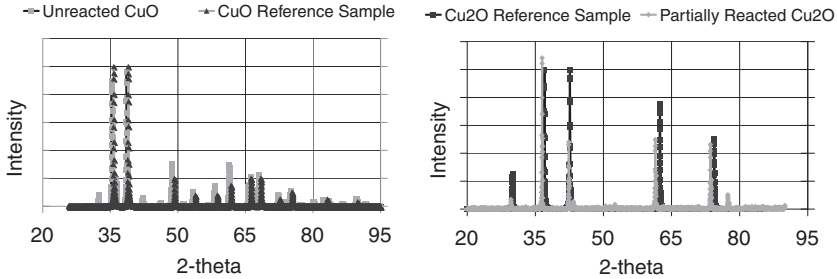

Fig. 2. XRD spectra of unreacted (left) and partially reacted (right) CuO particles.

Please cite this article in press as: E.A. Goldstein, R.E. Mitchell, *Proc. Combust. Inst.* (2010), doi:10.1016/j.proci.2010.06.080

limited overall conversion rates were used to determine the maximum specific conversion rates, $(1/m\ dm/dt)_{max}$. The measured specific conversion rates were smaller than these maximum rates. Based on the ratio of the actual (measured) and maximum specific conversion rates, the partial pressure of CO at the outer surface of the copper oxide particle was estimated, and the Thiele Modulus was calculated. In all cases the Thiele Modulus was of order one. No matter the order of reaction with respect to the CO partial pressure, the effectiveness factor was found to be greater than 0.90, indicative of particles being almost completely penetrated by CO. Consequently, in our analysis of the TGA data, we assume that there are no significant mass transport effects impacting the CuO and Cu_2O conversion rates and that the measured rates are limited primarily by the effects of chemical reaction. The CO concentration is assumed to be uniform inside the particles; reactions occur throughout the particle volumes.

4. Chemical reaction mechanism

An equilibrium analysis was performed in order to determine the temperature at which CuO starts to dissociate. This is relevant in determining the initiation chemical reaction pathways for copper oxide conversion. The results of the analysis indicated that for the gas environment of the TGA (nitrogen), CuO dissociation does not begin until about 873 K. The calculations also indicated that little Cu formation occurs at temperatures less than 1273 K; the CuO is thermally reduced primarily to Cu_2O at these temperatures. Since reactions between CuO and CO were found to commence at temperatures below the dissociation temperature of CuO, it was assumed that the reacting system was initiated by CO adsorption at copper sites within the solid CuO matrix. This was found to be true in a previous study by Wang et al. [10] in which they showed that CO adsorption follows a Langmuir–Hinshelwood type mechanism on Cu sites. In light of these assumptions, the following chemical reaction mechanism was developed to describe both the CuO/CO and Cu_2O/CO reacting systems:

$$CuO + CO \Longleftrightarrow CuO(CO) \quad (R.1)$$
$$CuO(CO) \rightarrow Cu + CO_2 \quad (R.2)$$
$$CuO + CuO(CO) \rightarrow Cu_2O + CO_2 \quad (R.3)$$
$$Cu_2O + CO \rightarrow Cu_2O(CO) \quad (R.4)$$
$$Cu_2O(CO) \rightarrow 2Cu + CO_2 \quad (R.5)$$
$$Cu_2O \Longleftrightarrow CuO + Cu \quad (R.6)$$
$$Cu + CO \Longleftrightarrow Cu(CO) \quad (R.7)$$
$$Cu + CuO(CO) \Longleftrightarrow CuO + Cu(CO) \quad (R.8)$$
$$Cu + Cu_2O(CO) \Longleftrightarrow Cu_2O + Cu(CO) \quad (R.9)$$

In these reactions, CuO(CO), Cu_2O(CO) and Cu(CO) are adsorbed surface species (copper sites having adsorbed CO) formed via reactions R.1, R.4 and R.7 when the copper species are exposed to CO. Reactions R.8 and R.9 are representative of migration reactions, where the loosely bound CO can diffuse on the surface between copper sites. These reactions are assumed to be reversible, as is reaction R.6. Reactions R.2, R.3 and R.5 represent desorption reactions, where an oxygen atom in the copper oxide matrix bonds with adsorbed CO forming CO_2, which escapes the particle surface. At temperatures greater than 873 K, a thermal decomposition reaction of the form: $2CuOCu_2O + 1/2O_2$ should also be included. Similar reaction pathways have been hypothesized by others [10,13,16] to explain the reduction process.

As a consequence of chemical reactions, the rate of change in the moles of species i is given by

$$\frac{dN_i}{dt} = \frac{d(S \cdot [X_i])}{dt} = [X_i] \cdot \frac{dS}{dt} + S \cdot \frac{d[X_i]}{dt} = S \cdot R\widehat{R}_i'' \quad (1)$$

where S is the total surface area (in m^2) available for adsorption, $[X_i]$ is the surface molar concentration of species i (in mol/m^2 for a surface species and mol/m^3 for a gas phase species), and $R\widehat{R}_i''$ is the overall reaction rate of species i per unit surface area (in mol/m^2). The surface molar concentrations $[X_i]$ (in mol/m^2) are determined as a function of the species site fractions, θ_i:

$$[x_i] = \frac{\theta \cdot (S_d/N_{AV})}{\eta_i} \quad (2)$$

where η_i is the number of sites that comprises species i (*e.g.*, Cu_2O comprises two Cu sites), S_d is the total surface site density (sites/m^2) and N_{AV} is Avogadro's number.

Equation (1) can be divided by the total surface area and combined with Eq. (2) to yield expressions for the rates of change in the site fractions during the course of reaction. These equations can be written in the following form when the overall reaction rates are written in terms of the net rates of the individual reactions:

$$\frac{d\theta_i}{dt} = \frac{\eta_i}{(S_d/N_{AV})} \sum_{j=1}^{9} \left(v'_{i,j} - v_{i,j}\right) \widehat{R}_j'' - \frac{\theta_i}{S}\frac{dS}{dt} \quad (3)$$

In the above expressions, the net rate of reaction j is given by

$$\widehat{R}_j'' = k_{fj} \prod_{i=1} [X_i]^{v_{i,j}} - k_{rj} \prod_{i=1} [X_i]^{v'_{i,j}} \quad (4)$$

where $v_{i,j}$ and $v'_{i,j}$ are the stoichiometric coefficients for species i in the forward and reverse directions, respectively, of reaction j, and k_{fi} and k_{ri} are the forward and reverse rate coefficients, respectively, of reaction j. For an irreversible reaction, $k_{rj} = 0$. We have allowed for the impact of surface area

Please cite this article in press as: E.A. Goldstein, R.E. Mitchell, *Proc. Combust. Inst.* (2010), doi:10.1016/j.proci.2010.06.080

change on the site fractions. In Cu oxidation, the surface area has been observed to decrease [18,19]; it is therefore reasonable to assume that during CuO reduction the surface area of the CuO and Cu_2O particles will change too.

It is assumed that the total surface area of a copper oxide particle depends on the relative amounts of the different species constituting the particle mass, as follows:

$$S = \sum_i \theta_i S_i = \sum_i \theta_i \cdot \frac{m_{init}}{\widehat{M}_{init} \cdot \eta_i} \cdot \widehat{M}_i \cdot S_{g,i}, \quad i = \mathrm{CuO}, \mathrm{Cu_2O}, \mathrm{Cu} \tag{5}$$

Here, m_{init} and $\widehat{M}_{init}$ are the total mass and molecular weight, respectively, of the copper oxide species initially placed on the TGA balance pan (either CuO or Cu_2O) and $S_{g,i}$ is the specific surface area (in g/m^2) of species i in the particle. Equation (5) can be differentiated with respect to time to yield an expression for dS/dt in terms of site fractions. When this expression is employed in Eq. (3), the resulting equations can be integrated simultaneously to yield the species site fractions as a function of time, for specified rate coefficients and initial conditions. For the presented calculations $S_{g,CuO} = 45\ m^2/g$, $S_{g,Cu2O} = 70\ m^2/g$ and $S_{g,Cu} = 95\ m^2/g$. The mass specific surface area for Cu_2O was estimated by averaging the mass specific surface area for CuO and Cu as was done by Mrowec [18]. When the initial mass is composed of CuO particles, instead of integrating Eq. (3) for the CuO site fraction, the CuO site fraction is determined by difference ($\theta_{CuO} = S_0/S - \theta_{Cu_2O} - \theta_{Cu} - \theta_{CuO}(CO) - \theta_{Cu_2O(CO)} - \theta_{Cu(CO)}$, where S_0 is the initial total surface area). When the initial mass is composed of Cu_2O particles, instead of integrating Eq. (3) for θ_{Cu_2O}, the Cu_2O site fraction is determined by difference. Having determined the site fractions, the surface concentrations and masses of each component in the particle are readily calculable.

Only those reactions that remove an oxygen atom from the bulk copper oxide matrix (producing CO_2) are considered to contribute to the intrinsic reactivity of the copper oxide to CO. As such, on a molar basis, the intrinsic chemical reactivity of CuO (or Cu_2O) to CO (the rate of oxidation of CO by the copper oxide) is given by

$$\widehat{R}''_{\text{Copper Oxide}} = \widehat{R}''_2 + \widehat{R}''_3 + \widehat{R}''_5 = (S_d/N_{AV})\left(k_2\theta_{CuO} + k_3(S_d/N_{AV})\theta_{CuO} \times \theta_{CuO(CO)} + \frac{1}{2}k_5\theta_{Cu_2O(CO)}\right) \tag{6}$$

This is the reduction rate of the copper oxide, which is also the overall formation rate of production of CO_2 (in $mol/m^2\ s$).

5. Experimental results and analysis

Thermogravimetric tests were undertaken to obtain data needed to determine the kinetic parameters that describe the reduction rates of CuO and Cu_2O when exposed to CO. Twenty to 30 mg of CuO or Cu_2O particles were placed in the TGA balance pan and weight was monitored in the conditions established in the TGA reaction chamber. For each experiment, the measured weight loss always corresponded to the complete conversion of the initial metal oxide to copper. Complete conversion was also independently verified through XRD analysis. After drag and buoyancy corrections, the weight-versus-time data were analyzed to determine as a function of time the quantity $1/m\ dm/dt$, a quantity that is proportional to the reaction rate. Based on the reaction mechanism presented above, this quantity depends on the rates of the chemical reactions as follows:

$$\left(\frac{1}{m}\frac{dm}{dt}\right)_{calc} = \left(-\widehat{M}_{CO}\widehat{R}''_1 + \hat{M}_{CO_2}\widehat{R}''_2 + \widehat{M}_{CO_2}\widehat{R}''_3 - \widehat{M}_{CO}\widehat{R}''_4 + \widehat{M}_{CO_2}\widehat{R}''_5 - \widehat{M}_{CO}\widehat{R}''_7\right)S_g \tag{7}$$

In this expression, S_g is the specific surface area of the particle ($S_g = S/m_{total}$), and the molar reaction rates are written in terms of rate coefficients k_i and the concentrations of the species involved in the reaction, as described above. Using a least squares procedure, k_i for each reaction was determined that minimized the sum of the differences in the measured and calculated values of $1/m\ dm/dt$ at each measurement time for each test performed.

Shown in Fig. 3 are results obtained when Cu_2O and CuO particles were placed on the TGA balance pan and the reactive gas consisted of 1.6% CO in nitrogen at temperatures ranging from 473 to 773 K. The conversion rate is observed to vary with time. Additionally, an induction time is observed that decreases with increasing temperature. An induction period has also been observed in previous work [9,10,13]. The calculated and measured conversion rate profiles are in adequate agreement; the model faithfully reproduces the trends observed experimentally. Arrhenius parameters that fit the reaction rate coefficients are presented in Table 1. The set is not unique. Other combinations of rate coefficients yielded nearly similar results; the values listed are the best in the least squares sense. The activation energies are in the range expected for adsorption/desorption type reactions, although on the low side. Reaction R.6 was found to be unimportant at temperatures less than 773 K. The Arrhenius parameters presented for reaction R.6 describe k_6 at 773 K for an arbitrarily selected activation energy of 80 kJ/mol.

Please cite this article in press as: E.A. Goldstein, R.E. Mitchell, *Proc. Combust. Inst.* (2010), doi:10.1016/j.proci.2010.06.080

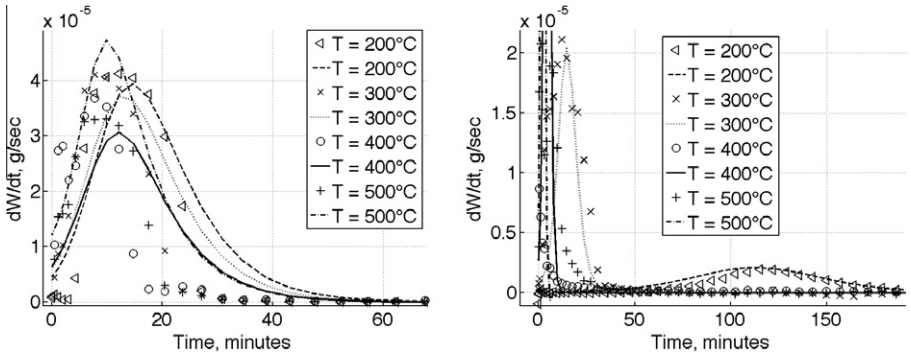

Fig. 3. Measured and calculated conversion rate profiles for (a) CuO and (b) Cu_2O particles exposed to 1.6% CO at selected temperatures (lines are calculations; points are measurements).

Table 1
Reaction mechanism and associated kinetic parameters.

Reaction	Forward rate coefficient		Reverse rate coefficient	
	A[a]	E (kJ/mol)	A	E (kJ/mol)
R.1 $CuO + CO \Leftrightarrow CuO(CO)$	4.01E−02	1.81E+01	3.83E+02	1.76E+01
R.2 $CuO(CO) \rightarrow Cu + CO_2$	3.10E+01	7.13E+00	[–]	[–]
R.3 $CuO + CuO(CO) \rightarrow Cu_2O + CO_2$	1.07E+07	6.03E+01	[–]	[–]
R.4 $Cu_2O + CO \rightarrow Cu_2O(CO)$	5.13E−01	3.42E+01	2.91E+02	1.57E+01
R.5 $Cu_2O(CO) \rightarrow 2Cu + CO_2$	4.27E+04	4.44E+01	[–]	[–]
R.6 $Cu_2O \Leftrightarrow CuO + Cu$	1.47E−10	8.00E+01	[b]	[b]
R.7 $Cu + CO \Leftrightarrow Cu(CO)$	1.49E+05	4.53E+01	8.49E+04	4.20E+01
R.8 $Cu + CuO(CO) \Leftrightarrow CuO + Cu(CO)$	3.25E+01	5.58E+00	2.11E+04	8.55E+00
R.9 $Cu + Cu_2O(CO) \Leftrightarrow Cu_2O + Cu(CO)$	1.61E+03	2.16E+01	3.10E+05	4.04E+01

[a] Units consistent with surface concentrations in mol/m^2 and time in s.
[b] Reverse rate calculated from equilibrium constant.

In order to obtain the agreement between measurements and calculations depicted in Fig. 3, it was necessary to introduce a scale factor that multiplies S_d, the copper oxide surface site density. Based on the crystalline structures, S_d for the copper oxides should be in the range 10^{19}–10^{20} copper sites per square meter of projected surface. In our calculations, a value of 2.81×10^{21} was used, suggesting the involvement of bulk copper sites in the experiments.

In order to determine the influence of each reaction in the mechanism, a sensitivity analysis was performed. Each reaction rate coefficient was perturbed by ±5%, in turn, and the time for 90% conversion (τ) was calculated. Reaction sensitivity was defined as:

$$S_{R\cdot i} = \frac{\partial \tau}{\partial k_i}\frac{k_{i\cdot 0}}{\tau} \approx \left(\frac{\tau_{1.05k_i} - \tau_{0.95k_i}}{\tau_{k_i}}\right)\left(\frac{k_i}{1.05k_i - 0.95k_i}\right) \quad (8)$$

Sensitivity values determined at four conditions (200 °C and 500 °C for pure CuO particles exposed to 1.6% CO in N_2 and 5.0% CO in N_2) are shown in Fig. 4. A negative sensitivity implies that increasing the rate coefficient decreases the 90% conversion time or that decreasing the rate coefficient increases the conversion time. The analysis indicates that in all the cases considered, the 90% conversion times are most sensitive to the CO adsorption and migration reactions (reactions R.7 and R.8, respectively). At 200 °C, the conversion times are relatively insensitive to reaction R.3 but as temperature is increased, the reaction becomes activated, producing Cu_2O. As a result, as temperature is increased, the 90% conversion times become sensitive to reactions R.4, R.5 and R.9, providing pathways for Cu_2O reduction to elemental copper. This explains the cascading pathway for CuO reduction in CO environments observed when temperatures are high [13]. Additionally, a similar sensitivity analysis indicates that the induction time is most influenced by the migration reactions, R.8 and R.9.

6. Discussion

The kinetic model was used to examine some of the characteristics of copper oxide reduction in CO environments. Under atmospheric conditions, the

Please cite this article in press as: E.A. Goldstein, R.E. Mitchell, *Proc. Combust. Inst.* (2010), doi:10.1016/j.proci.2010.06.080

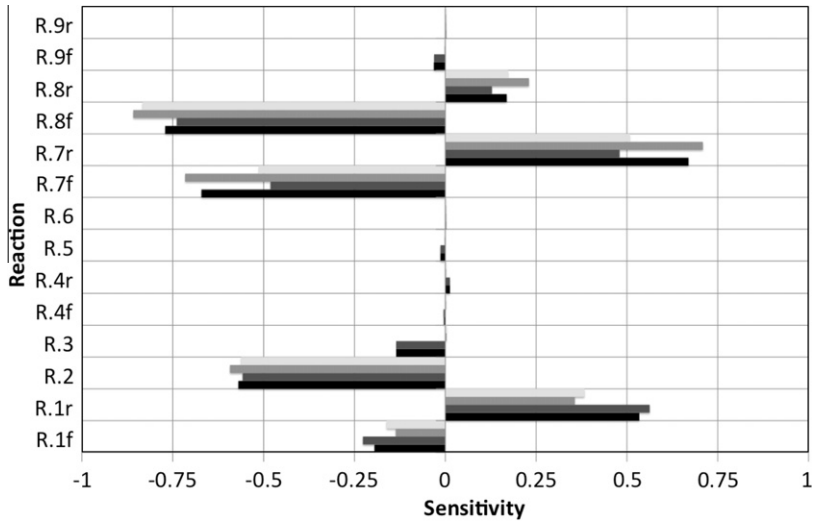

Fig. 4. CuO conversion sensitivity to ±5% changes in reaction rate coefficients. *Gas conditions*: ■ 500 °C, 1.6% CO in N_2, ■ 500 °C, 5.0% CO in N_2, ■ 200 °C, 1.6% CO in N_2, ■ 200 °C, 5.0% CO in N_2.

dependences of the copper oxide reduction rate on the CO mole fraction and on temperature are shown in Fig. 5. At fixed temperature, as the CO mole fraction is increased, the rate of oxygen release from the copper oxide matrix is increased. The model supports a reaction order with respect to the CO partial pressure of 0.7, as indicated by the slopes of the lines in the figure. At fixed CO mole fraction, as the temperature is increased, the oxygen release rate also increases as expected. Similar observations were made by Wang [13]. Overall activation energies of 20 and 25 kJ/mol are estimated for CuO and Cu_2O reduction, respectively, to Cu, as indicated by the slopes of the lines in the left panel of Fig. 5. Other publications also have reported higher activation energies for Cu_2O reduction when compared to CuO reduction [15,24]. In similar TGA experiments performed with particles consisting of 10% CuO in Al_2O_3 exposed to a range of CO concentrations at 723–1223 K, an overall activation energy of 14 kJ/mol and a reaction order with respect to the CO concentration of 0.8 has been reported for CuO reduction [25,26]. An overall activation energy of 28 kJ/mol for CuO reduction has been reported with particles consisting of 82.5% CuO in Al_2O_3 exposed to 10% CO (balance N_2) at temperatures up to 1223 K [24].

Calculations indicate that as the total pressure is increased, the copper oxide reduction rate increases, rather rapidly between zero and 1 atm but very slowly between 1 and 100 atm. At 400 °C, between 1 and 100 atm, the overall conversion rate varies with total pressure to the 0.80 power for Cu_2O and the 0.3 power for CuO.

Calculations also indicate that when temperatures are greater than about 300 °C, the reduction sequence is CuO to Cu_2O to Cu. At the higher

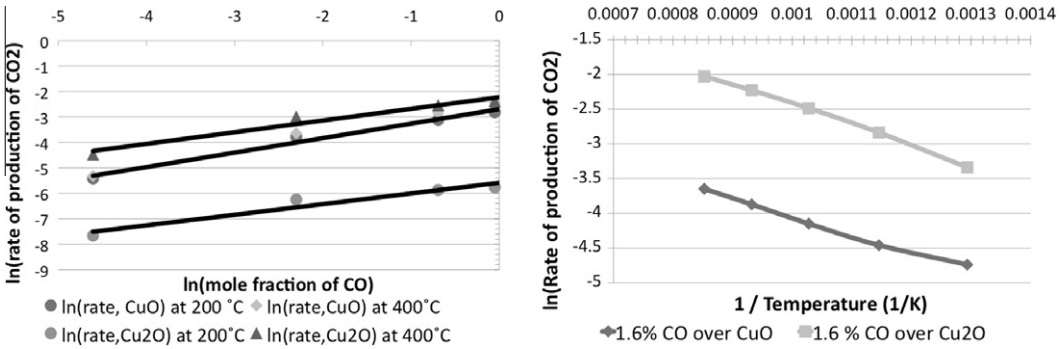

Fig. 5. Calculated conversion rates for a CuO particle exposed to various CO environments at selected temperatures (left) and calculated overall conversion rates for a CuO particles exposed to 1.6% CO at selected temperatures (right).

Please cite this article in press as: E.A. Goldstein, R.E. Mitchell, *Proc. Combust. Inst.* (2010), doi:10.1016/j.proci.2010.06.080

temperatures, reaction R.3 becomes more important, opening a channel for Cu_2O formation. At low temperature, the direct path to Cu formation is dominant. These findings are consistent with the results of previous investigators [10,13,16,17].

7. Conclusions

The results of our experimental and modeling efforts indicate that copper I (Cu_2O) and copper II (CuO) oxides are ideal oxygen carriers for chemical looping combustion applications. The experiments support the thermochemical equilibrium calculations that indicate that the CuO is relatively stable at temperatures below 873 K in inert environments, higher temperatures being required for release of oxygen. With CO in the ambient gas, CO_2 is observed at temperatures as low as 473 K, indicating that the reactive gas initiates copper oxide decomposition. At temperature conditions in excess of 873 K, a thermal decomposition reaction should be included in the mechanism.

A model for a CuO or Cu_2O particle undergoing chemical reaction when exposed to a CO environment was developed that accounts for the changes in mass that particles undergo as oxygen is released from the solid matrix. Reaction is initiated by the adsorption of CO at copper sites within the solid. Migration of CO on the surface is important in determining both the initial induction time as well as the overall reduction time. The reduction pathway can either cascade through CuO to Cu_2O to Cu or be direct (CuO to Cu), the direct route being dominant at low temperatures.

With the kinetic parameters determined, overall copper oxide reduction rates are influenced by mass transport effects at temperatures in excess of 873 K for particles larger than 125 μm. Consequently, the combined effects of chemical reaction and mass transport must be considered when predicting CuO reduction rates in environments likely to be established in the fuel reactor of a chemical looping combustion system.

Acknowledgements

The authors would like to acknowledge the support from the California Energy Commission Grant 07-01-37 and Clean EnGen L.L.C.

References

[1] M. Mellish, D. Kearney, S. Kette, *International Energy Outlook 2009*, U.S. Energy Information Administration, 2009.
[2] M.M. Hossain, H.I. de Lasa, *Chem. Eng. Sci.* 63 (18) (2008) 4433–4451.
[3] A. Abad, T. Mattisson, A. Lyngfelt, M. RydÈn, *Fuel* 85 (9) (2006) 1174–1185.
[4] Y. Cao, W.P. Pan, *Energy Fuels* 20 (5) (2006) 1836–1844.
[5] L.F. de Diego, F. GarcÌa-Labiano, J. Adnez, et al., *Fuel* 83 (13) (2004) 1749–1757.
[6] F. GarcÌa-Labiano, L.F. de Diego, J. Adnez, A. Abad, P. Gayn, *Chem. Eng. Sci.* 60 (3) (2005) 851–862.
[7] M. Ishida, M. Yamamoto, T. Ohba, *Energy Convers. Manage.* 43 (9–12) (2002) 1469–1478.
[8] G. Touchton, M. Zuzga, *Air Independent Internal Oxidation Steam Generator*, Final Report, California Energy Commission, 2009.
[9] J.A. Rodriguez, J.Y. Kim, J.C. Hanson, M. Pérez, A.I. Frenkel, *Catal. Lett.* 85 (3) (2003) 247–254.
[10] J.B. Wang, D.-H. Tsai, T.-J. Huang, *J. Catal.* 208 (2) (2002) 370–380.
[11] W.-P. Dow, T.-J. Huang, *J. Catal.* 160 (2) (1996) 171–182.
[12] W.-P. Dow, Y.-P. Wang, T.-J. Huang, *J. Catal.* 160 (2) (1996) 155–170.
[13] X. Wang, J.C. Hanson, A.I. Frenkel, J.-Y. Kim, J.A. Rodriguez, *J. Phys. Chem. B* 108 (36) (2004) 13667–13673.
[14] X. Tang, B. Zhang, Y. Li, Y. Xu, Q. Xin, W. Shen, *Catal. Today* 93–95 (2004) 191–198.
[15] J.Y. Kim, J.A. Rodriguez, J.C. Hanson, A.I. Frenkel, P.L. Lee, *J. Am. Chem. Soc.* 125 (35) (2003) 10684–10692.
[16] M.x. Moreno, L. Bergamini, G.T. Baronetti, M.A. Laborde, F.J. MariÒo, *Int. J. Hydrogen Energ.* 35 (11) (2010) 5918–5924.
[17] A. MartÌnez-Arias, D. Gamarra, M. Fern ndez-GarcÌa, A. HornÈs, P. Bera, Z. Kopp ny, Z. Schay, *Catal. Today* 143 (3–4) (2009) 211–217.
[18] S. Mrowec, A. Stokłosa, *Oxid. Metals* 3 (3) (1971) 291–311.
[19] K. Mimura, J.-W. Lim, M. Isshiki, Y. Zhu, Q. Jiang, *Metall. Mater. Trans. A* 37 (4) (2006) 1231–1237.
[20] S. Brunauer, P.H. Emmett, E. Teller, *J. Am. Chem. Soc.* 60 (2) (1938) 309–319.
[21] S.J. Gregg, K.S.W. Sing, H.W. Salzberg, *J. Electrochem. Soc.* 114 (11) (1967) 279C.
[22] N. Tsai, *Influence of High CO Concentration on the CO_2 Gasification of a Selected Coal Char*, Ph.D. Thesis, Stanford University, Stanford, CA, 1998.
[23] R.E. Mitchell, R.H. Hurt, L.L. Baxter, D.R. Hardesty, *Compilation of Sandia Coal Char Combustion Data and Kinetic Analyses*, Milestone Report, SAND-92-8208, 1992.
[24] S.Y. Chuang, J.S. Dennis, A.N. Hayhurst, S.A. Scott, *Proc. Combust. Inst.* 32 (2) (2009) 2633–2640.
[25] F. Garcia-Labiano, J. Adanez, L.F. deDiego, P. Gayan, A. Abad, *Energy Fuels* 20 (1) (2006) 26–33.
[26] F. Garcia-Labiano, L.F. de Diego, J. Adanez, A. Abad, P. Gayan, *Ind. Eng. Chem. Res.* 43 (26) (2004) 8168–8177.

Please cite this article in press as: E.A. Goldstein, R.E. Mitchell, *Proc. Combust. Inst.* (2010), doi:10.1016/j.proci.2010.06.080